Silica Functionalized Magnesium Ferrite Nanocomposites for Potential Biomedical Applications: Preparation, Characterization and Enhanced Colloidal Stability Studies

Ehi-Eromosele C.O.[1,a*], Ita B.I.[1 & 2,b], Iweala E.EJ.[3,c], Ogunniran K.O. [1,d], Adekoya J.A.[1,e], Siyanbola T.O. [1,f]

[1]Department of Chemistry, Covenant University, PMB 1023, Ota, Nigeria.
[2]Department of Pure and Applied Chemistry, University of Calabar, Calabar, Nigeria.
[3]Department of Biological Sciences, Covenant University, PMB 1023, Ota, Nigeria.
[a]cyril.ehi-eromosele@covenantuniversity.edu.ng, [b]iserom2001@yahoo.com,
[c]emeka.iweala@covenantuniversity.edu.ng, [d]kehinde.ogunniran@covenantuniversity.edu.ng,
[e]joseph.adekoya@covenantuniversity.edu.ng, [f]tolutope.siyanbola@covenantuniversity.edu.ng

Abstract. Magnetic nanocomposite material composed of silica coated $MgFe_2O_4$ for potential biomedical applications were synthesized by a two-step chemical method including solution combustion synthesis, followed by silica coatings of the ferrite nanoparticles. The effects of silica coatings on the structural, morphological and magnetic properties were comprehensively investigated using powder X-ray diffraction (XRD), Field Emission Scanning Electron Microscope (FESEM), energy dispersive absorption x-ray (EDAX), Fourier Transform Infrared spectroscopy (FTIR), thermogravimetric analysis and differential thermal analysis (TG–DTA) and vibrating sample magnetometer (VSM). The colloidal behaviour of coated MNPs in physiological saline medium like water or phosphate buffer saline (PBS) was also studied by zeta potential measurements. The XRD patterns indicate that the crystalline structure is single cubic spinel phase and the spinel structure is retained after silica coating. Also, after silica coating, the crystallite size (from Scherrer formula) decreases from 53 to 47 nm. The magnetic results show that $MgFe_2O_4$ MNPs (bare and silica coated) is ferrimagnetic at room temperature. Zeta potential studies revealed that there is enhanced colloidal stability of $MgFe_2O_4$ MNPs after silica coating in aqueous media which is an applicable potential in biomedical applications.

1.0 Introduction

In the last two decades, a number of nanoparticle-based therapeutic and diagnostic agents have been developed for the treatment of cancer, diabetes, pain, asthma, allergy, infections, and so on [1,2] (Brannon-Peppas and Blanchette, 2004; Kawasaki and Player, 2005). Magnetic nanoparticles (MNPs) have attracted great interest in a number of biomedical applications due to their inherent magnetic properties and biocompatibility [3]. The functional properties of these MNPs can be tailored for specific biological functions, such as drug delivery [4,5], hyperthermia or magnetic targeting [6,7], magnetic resonance imaging (MRI) [8,9], cell labeling and sorting [10,11], and immunoassays [12].

The spinel ferrite ferromagnetic or superparamagnetic nanomaterials with general formula MFe_2O_4 (M = Mn, Fe, Ni, Co, Zn, Mg) are currently under extensive development in advanced therapeutics and diagnosis of a wide range of diseases. Typically, they have been used as heating foci in hyperthermia, contrast agents in MRI and magnetic field-guided drug delivery [5,13-15]. The structural and magnetic properties of spinel ferrites strongly depend on magnetic moment, particle size and distribution, shape and crystallinity which are highly sensitive to method of preparation [16,17]. Various methods of synthesis such as ball milling, co-precipitation, sol-gel, reverse micelle, hydrothermal and combustion methods have been used for the synthesis of $MgFe_2O_4$ nanoparticles [18-22]. Most of the wet chemical methods like chemical co-precipitation and hydrothermal require careful control of pH of the solution, temperature, time and concentration

like parameters for formation of particles. Combustion method offers mass production, low processing time, cost effectiveness, good stoichiometric control and ultrafine particle formation with narrow size distribution, which has an important influence on the magnetic properties of the ferrite.

MNPs tend to aggregate due to the strong dipole–dipole interaction and lack of surfactants. They are chemically very active and, in most cases, become surface oxidized when exposed to air. Hence, the modification of the surface of the MNPs with biocompatible and biodegradable materials (inorganic, organic or polymeric) is required for biomedical applications [23,24]. Different materials like polyethylene glycol, polyvinyl alcohol, oleic acid, dextran, chitosan, gold, silica etc. have been used for the surface modification of MNPs, in order to improve their biocompatibility and colloidal stability. Silica has been widely used as a coating material for MNPs used in biomedical applications [25,26]. Its biocompatibility, stability against degradation, and easy surface modification due to the abundant silanol groups, is making silica microspheres of particular interest for use in biomedicine and bioengineering [27].

Magnesium-based nanoparticles have been used as a potential agent in several biological applications. They have been shown to have antibacterial [28,29] and antitumoral activities [30]. Nanocrystalline $MgFe_2O_4$ has also been investigated as potential heating agents in magnetic hyperthermia [31]. None of these reports have investigated the surface modification of nanocrystalline $MgFe_2O_4$ even though it is a requirement for biological applications. Even though there is a multitude of known magnetic materials with potentials for biomedical applications, their biomedical applicability has been restricted by the strict demand of biocompatibility. Also, the magnetic structure of the surface layer usually is greatly different from that in the body of nanoparticle, and the magnetic interactions in the surface layer could have a notable effect on the magnetic properties of nanoparticles [32]. Hence, the interaction between the surfactant and the nanoparticle is critical and essential to synthesis and application of nanoparticles [33]. Therefore, the current study is about the solution combustion synthesis of nanocrystalline $MgFe_2O_4$ using a mixture of fuel (urea and ammonium acetate) approach, subsequently subjected to a size selection process, and coated with silica. The effect of silica coatings on the structural, morphological and magnetic properties are discussed in detail. The colloidal stability of bare and silica coated $MgFe_2O_4$ MNPs in water was examined. The colloidal stability of silica coated $MgFe_2O_4$ MNPs in phosphate buffer solution (PBS) at pH 7.4 (physiological pH) and pH 5.0 (cancer cell endosomal pH) was also studied to test its colloidal stability under biorevelant conditions highlighting its potential *in-vivo* biomedical applications e.g., magnetic hyperthermia and targeted drug delivery.

2.0 Experimental

2.1 Materials
Analytical grade $Mg(NO_3).6H_2O$ (99% purity of Alfar Aesar), $Fe(NO_3)_3.9H_2O$ (99% purity of Sigma Aldrich), urea (U, CH_4N_2O) and ammonium acetate (AA, CH_3COONH_4) obtained from SD Fine Chem. Ltd., Mumbai were used as starting materials. Tetraethoxy silane (TEOS), ethanol and ammonia solution (ammonium hydroxide solution, ca 25% NH_3) were Sigma Aldrich, Germany products. Double distilled water was used throughout the experiments. All reagents were used without further purification.

2.2 Synthesis of $MgFe_2O_4$ MNPs
$MgFe_2O_4$ MNPs were prepared by the solution combustion method using urea and ammonium acetate as fuels. The optimization of the crystallinity and particle size of $MgFe_2O_4$ MNPs using a mixture of fuels has been studied in detail in our recent publication [34]. Stoichiometric amounts of $Mg(NO_3).6H_2O$, $Fe(NO_3)_3.9H_2O$, CH_4N_2O and CH_3COONH_4 were dissolved in 20 ml of de-ionised water. Then the solutions were heated to 80^oC to form a viscous gel of precursors under magnetic stirring. Secondly, the gel is transferred to a pre-heated coil (300^oC). Finally, after a short moment,

the solution precursors boiled, swelled, evolved a large amount of gases and ignited, followed by the yielding of puffy black products. Part of this final product (auto-combustion powder) was annealed at 900°C for 2hrs each to obtain a pure nanocrystalline ferrite phase. In order to disaggregate the MNPs and select the smaller ones, a procedure reported by Villanueva et al [26] was performed with slight modifications. The MNPs (900 mg) were dispersed in ethanol (200 mL), and the solution was ultrasonicated at 60°C for 2 hrs. Then, the suspension was taken out from the bath and left at 100°C with reflux for 24 hrs. The solution was allowed to settle at room temperature for 24 hrs. The largest particles tended to aggregate and settled at the bottom of container and they were collected with the help of a magnet. The particles that still remain dispersed in the solution which are the smallest ones were collected by centrifugation and dried at 60°C and then used for further silica coating.

2.3 Synthesis of Silica Coated MNPs
The MNPs were coated with silica following the Stober method [35]. The MNPs (100 mg) were added to a solution of 150 mL of ethanol that contained distilled water (10 mL) and ammonium hydroxide (2 mL). The solution was maintained in an ultrasonic bath for 1 hr. Then, tetraethoxy silane (TEOS) (2 mL) was added to the solution and sonicated for 15 min. This process was repeated twice. Finally, the mixture was allowed to stand for 24 hrs. The solution was filtered and the NPs were washed with ethanol five times and dried at 60°C in the oven.

2.4 Physico-Chemical Characterization
The X-ray diffractograms of the bare and silica coated MNPs were recorded using an X-ray diffractometer (D8 Advance, Bruker, Germany), equipped with a Cu Kα radiation source (λ = 1.5406 A˚) and the crystallite size was calculated by the well-known Debye-Scherrer relation.

$$D = \frac{0.9\lambda}{\beta Cos\theta}$$

(1)

where β is the full-width at half maxima (in radians) of the strongest intensity diffraction peak (311), λ is the wavelength of the radiation and θ is the angle of the strongest characteristic peak. Eq. 2. was employed to calculate the lattice parameter (a) using the value of d-spacing of the strongest intensity diffraction peak.

$$a = d_{hkl}\sqrt{h^2 + k^2 + l^2}$$

(2)

where, h, k, l are the Miller indices of the crystal planes and d_{hkl} is the separation of lattice planes X-ray density (D_x) was calculated using equation 3.

$$D_X = \frac{8M}{Na^3}$$

(3)

Where, M is the molecular weight, N is the Avogadro's number, and a, is the lattice constant. The surface morphology and elemental detection were examined with a Field Emission-Scanning Electron Microscopes, Nova Nano SEM 600 (FEI Co., Netherlands). Thermal decomposition behavior of silica coated MNPs was carried out in a temperature range of 30-1000°C in argon atmosphere with a heating rate of 10°C/min using STA 409 PC Luxx from NETZSCH-Geratebau (Germany). The silica coating was investigated by using Fourier Transform Infrared spectroscopy (ALPHA, Bruker) in the range of 400 to 4000 cm^{-1}. The magnetic characterizations were carried out with a Vibrating Scanning Magnetometer (Lake Shore cryotronics-7400 series) under the applied field of ±20,000 G at room temperature. Zeta potential measurements were performed using a zeta sizer (Nano Zs, Nano series Malvern instruments). Measurements were taken in water and in PBS. Zeta potential measurements were done thrice for each sample at 30 electrode cycles.

3.0 Results and Discussion
3.1 Silica Coating of Polycrystalline MgFe$_2$O$_4$

In order to improve the safety aspects of their biomedical applications, surface modification of MNPs is necessary. The coating of MgFe$_2$O$_4$ core with a biocompatible inorganic material was used to passivate the MNP surface and also to improve the colloidal stability. Silica coatings on nanoparticles provide a rich surface chemistry, high biocompatibility and an anomalously high stability, especially in aqueous media. It is assumed that silica adsorbed on the surface of magnetic core of MgFe$_2$O$_4$ MNPs and forms a shell. The graphical representation of the size selection and silica coating procedure is shown in Fig. 1. Before coating of the MgFe$_2$O$_4$ core, a size selection of the agglomerated polycrystalline MgFe$_2$O$_4$ MNPs was done. The particles obtained by the combustion method using both urea and a mixture of fuel produced agglomerates due to the dipolar magnetic interaction and the lack of surfactants used in the synthesis. In spite of the lack of homogeneity in size, the combustion method assures chemical homogeneity of the sample. Since dipolar magnetic interactions decreases with increase in temperature, this is used to disaggregate the sample. When particles are dispersed in ethanol, sonicated and heated, aggregates are broken, producing more isolated nanoparticles of smaller sizes [26].
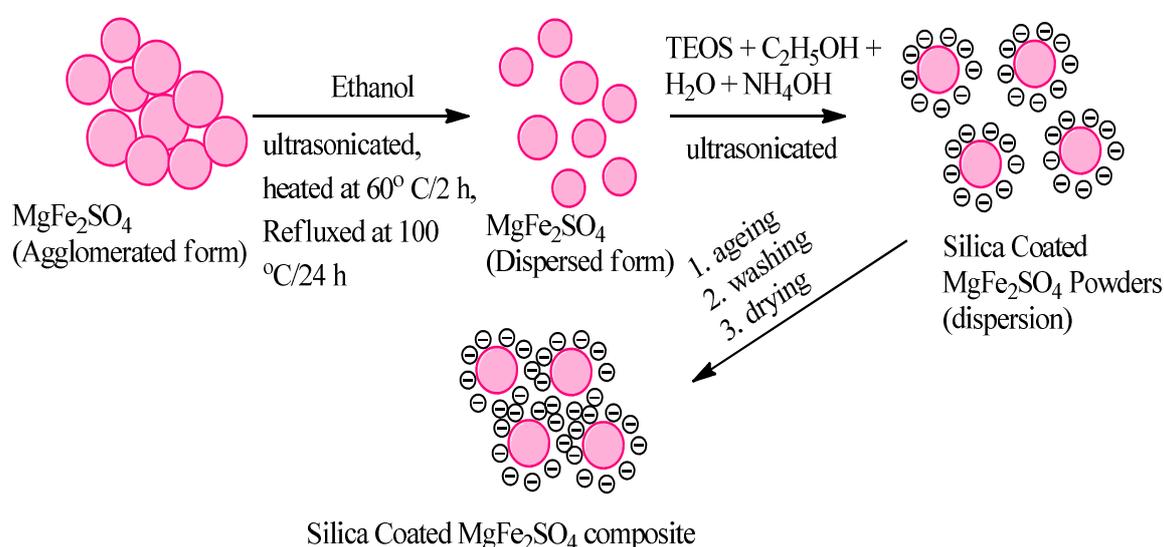
Fig. 1: Schematic Representation of the Size Selection and Silica Coating of MgFe$_2$SO$_4$ Processes

3.2 Structural and Phase Analysis

XRD was performed on the bare (sample not coated with silica i.e. the powder before size selection was done) and silica coated samples of nanocrystalline MgFe$_2$O$_4$ and it is shown in Fig. 2. The effects of size selection and silica coating on the structural properties of MgFe$_2$O$_4$ MNPs are presented in Table 1. Like the XRD of the bare sample, the coated sample showed all the characteristic peaks of spinel cubic structure (JCPDS card no. 73-1720) in the diffraction pattern. This clearly showed that the sample retained the spinel structure even after coating by silica but with a slight suppression of diffraction peaks. Therefore, the XRD data suggests that the silica shell consists mainly of amorphous phase rather than polycrystalline one [36] since there is the absence of silica-derived diffraction peaks. There is a pronounced change in the calculated structural properties of the coated sample compared to the bare sample with the coated sample recording lesser values of lattice parameter (a) and unit cell volume (V) but higher X-ray density (D$_x$) value than the bare sample. The calculated crystallite sizes (D) for the bare sample and the coated sample are 53 nm and 47 nm, respectively (Table 1). The reduction in the calculated crystallite size which had also caused the reduction in other structural properties might be due to the size selection process done to disaggregate the particles. Some researchers have reported the reduction in the crystallite size of nanoparticles after coating [37]. The changes in the structural properties of the coated sample might also be due to the silica coating.

Fig. 3 shows typical FE-SEM images of bare and silica coated $MgFe_2O_4$ MNPs. From Fig. 3, it can be observed that the bare sample is in highly agglomerated form whereas the coated sample displays better dispersion. The image for the coated sample shows clusters of MNPs as silica like most coatings can coat single particles and aggregates. However, there is reduced agglomeration, confirming the presence of silica coating on the MNPs; which helps to reduce the magnetic interactions between nanoparticles. The nanoparticles after silica coatings retained the faceted structure of uncoated samples but had a fairly lesser regular near-spherical structure compared with the bare sample. In addition, Fig. 4 shows the EDAX spectrum for the silica coated $MgFe_2O_4$ MNPs. The spectrum contained four peaks (carbon peak is probably due to sample holder), which were assigned to Mg, Fe, O, and Si. The peak of Si confirms the association of silica on the surface of $MgFe_2O_4$ MNPs. Therefore, the EDAX analysis suggests Mg, Fe, O, and Si are the main constituents in the nanocomposite.
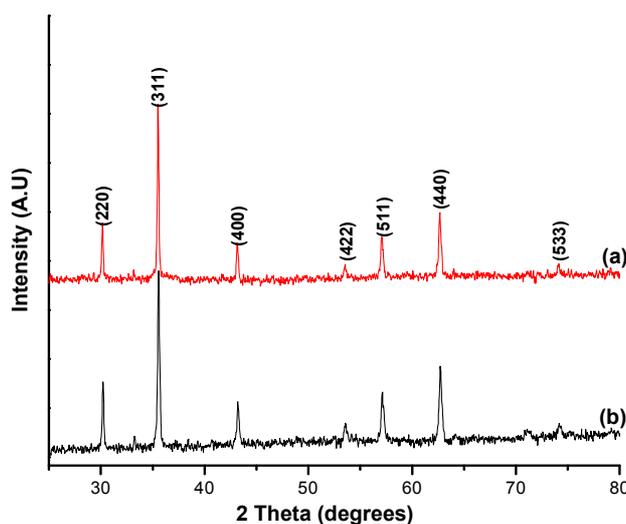
Fig. 2: X-ray diffraction patterns of polycrystalline $MgFe_2O_4$ (a) bare and (b) silica coated samples

Table 1: Effects of Size Selection and Silica Coating on the Structural Properties of $MgFe_2O_4$ MNPs

$MgFe_2O_4$	Crystallite size, D, (nm)	Lattice constant, a, (nm)	Unit cell volume, V, nm^3	X-ray density, D_x, g/cm^3
Bare	53	0.838	0.5885	4.5147
Coated	47	0.837	0.5864	4.5309
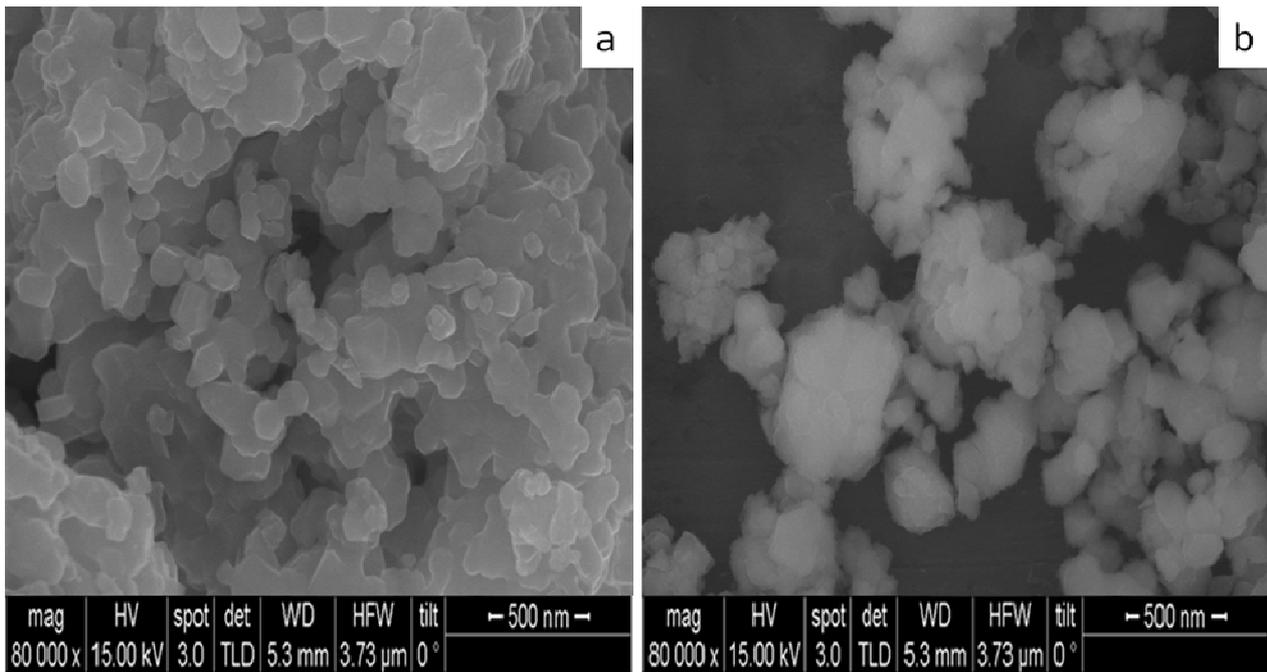
Fig. 3: FESEM images of polycrystalline MgFe$_2$O$_4$ (a) bare and (b) silica coated samples

Element	Atomic %
O	52.8
Mg	16.95
Si	2.13
Fe	28.12
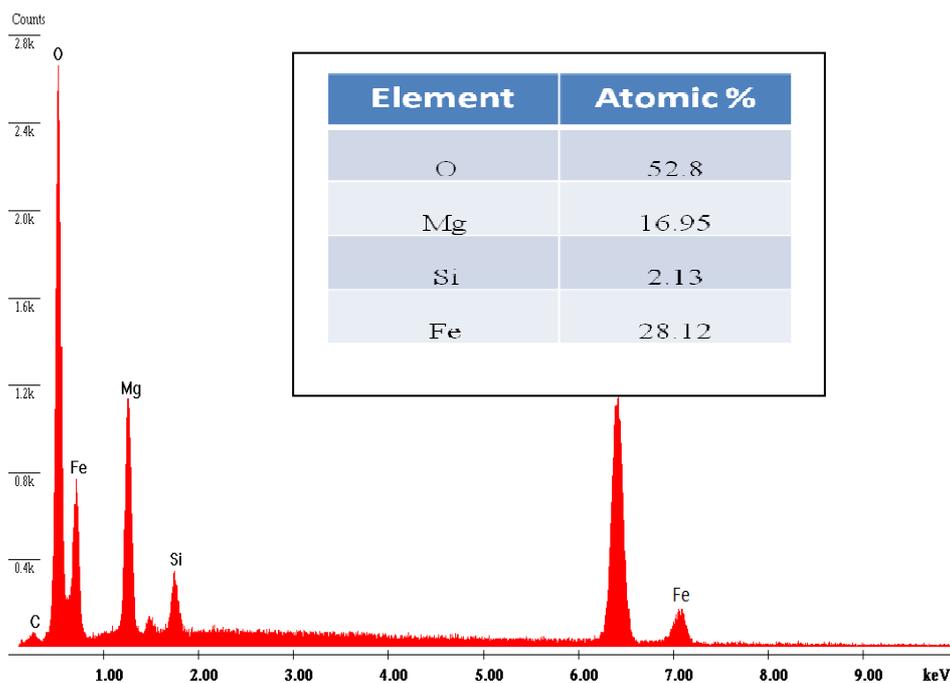
Fig. 4: EDAX spectra of silica coated MgFe$_2$O$_4$ nanocomposite

Fig. 5 shows the FTIR spectra of the bare and the coated sample. FTIR is an appropriate technique to confirm the attachment of silica to the surface of the MNPs. In case of the bare sample, the band observed at 560 cm^{-1} corresponds to stretching vibrations of Fe−O which is a typical metal–oxygen absorption band for the spinel structure of the ferrite [38,39]. In the coated sample, there is a shift of the stretching vibrations of Fe−O to 574 cm^{-1} which might be due to the silica coating and confirms the presence of the ferrite nanoparticles in the silica nanocomposite. The characteristic absorption band at 430 cm^{-1} and 1077 cm^{-1} corresponds to the bending and stretching vibrations of Si-O-Si, respectively which confirm the formation of SiO$_2$ [40,41]. Therefore, the formation of ferrite and attachment of silica onto MgFe$_2$O$_4$ MNPs surface is confirmed and supported by FTIR analysis.
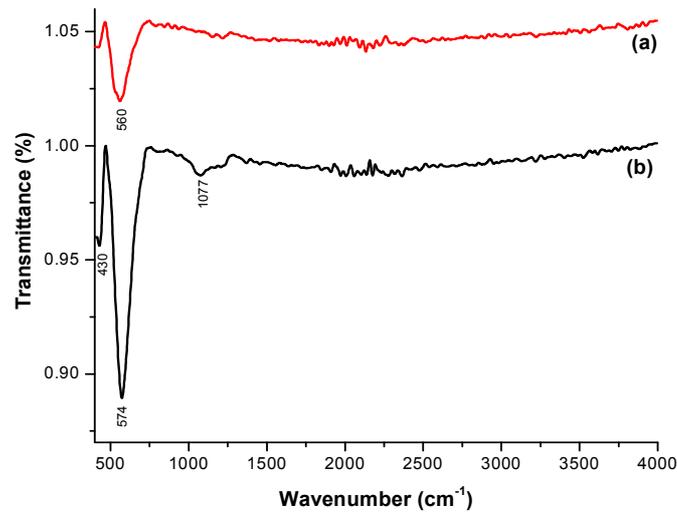
Fig. 5: FTIR spectra of (a) bare MgFe$_2$O$_4$ (b) silica coated MgFe$_2$O$_4$

3.3 Thermal analysis

Thermogravimetric analysis (TGA) can provide additional quantitative evidence on the structure of the nanoparticle coatings. It is an extremely valuable technique for surface characterization of nanoparticles. TGA allows us to determine the bonding strength of the ligand to the nanoparticle surface and its chemical stability [37]. The results of simultaneous thermal analysis - TGA and DTA (differential thermal analysis), on the silica coated MgFe$_2$O$_4$ MNPs are presented in Fig. 6. The weight loss process is observed in two stages. In the first, ~20% weight loss (which might be due to the vapourisation of residual moisture) in the temperatute range of 30 - 120°C corresponds to the endothermic peak (appearing as a kink) at about 120°C. However, in the 120 - 155°C temperature range, ~75% weight loss (corresponding to a sharp endothermic peak at ~150°C in the DTA curve) is noticed in the second stage which was attributed to the detachment of coated silica layer from the surface. It is well known that SiO$_2$ synthesized by the Stöber process possess high amounts of water and ethanol adsorbed on the surface, and both are removed by heating up to 150-200°C [42,43]. This might have accounted for the high weight loss associated with the detachment of silica coatings. It can also be seen that in the 155-1000°C temperature range, no significant weight loss is observed confirming the presence of pure MgFe$_2$O$_4$ phase. From this analysis, a high amount of silica is attached to nanoparticles' surfaces which also confirm the presence of silica on the surface of MNPs. The results also show the potential stability of the silica coated sample in applications less than 155°C.
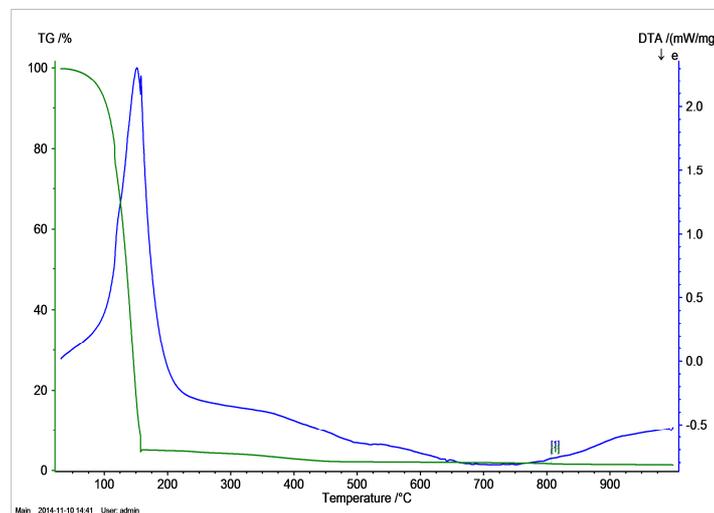
Fig 6: TG-DTA curves silica coated MgFe$_2$O$_4$ MNPs

3.4 Magnetic Studies

The hysteresis loops measured at room temperature for the bare and silica coated $MgFe_2O_4$ samples are shown in Fig. 7. The magnetic results show that $MgFe_2O_4$ MNPs (bare and silica coated) is ferrimagnetic at room temperature. The saturation magnetization (M_s), remanence (M_r), coercivity (H_c) and loop squareness ratio (M_r/M_s) of the bare and coated sample were summarized in Table 2. It can be seen that the M_s of the coated sample (22 emu/g) is smaller when compared to the bare sample (26 emu/g) at an applied field of ±20,000 G at 300 K. However, the magnetization for both samples is close to that of the bulk $MgFe_2O_4$ MNPs (~30 emu/g) [44]. $MgFe_2O_4$ is a mixed type spinel ferrite with the Mg^{2+} and Fe^{3+} metal ions distributed over the tetrahedral and octahedral sites. $MgFe_2O_4$ is an interesting magnetic material where magnetic couplings purely originate from the magnetic moment of Fe cations and may be relatively weaker due to non magnetic Mg^{2+} metal ions [45]. The reduction in magnetization for the coated sample may be attributed to the presence of non-magnetic silica layer on the surface of MNPs which reduces the particle-particle interaction and lowers the exchange coupling energy which in turn reduces the magnetization [37]. The reduction in magnetization might also be due to the lesser amount of magnetic substance per gram in the silica coated sample compared with the bare sample [5]. A reduction in magnetization was also reported for silica coated LSMO particles [25]. The coated sample had a lesser M_r, but a higher H_c and M_r/M_s values than the bare sample. M_s, M_r, and H_c are important magnetic properties critical to biomedical applications. The M_r/M_s for both the bare and coated samples is found to be higher than 0.5 which is the expected value for randomly packed single domain particles [46]. The alternating current susceptibility measurements of the coated sample showed that the magnetic responses are frequency dependent which is an important parameter in hyperthermia and targeted drug delivery applications [7,47].
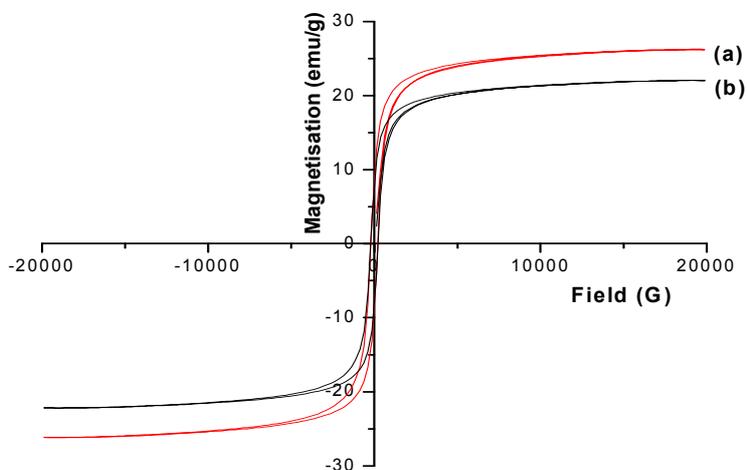
Fig. 7: Magnetic hysteresis curves of MgFe₂O₄ measured at room temperature for (a) the bare sample (b) silica coated sample

Table 2: Magnetic Properties of the Uncoated and the Silica Coated MgFe₂O₄

Sample	Saturation Magnetisation, M_s (emu/g)	Remanence Magnetisation, M_r (emu/g)	Coercivity (Gauss)	M_r/M_s
Bare sample	26	15	198	0.58
Silica coated sample	22	13	215	0.59

3.5 Colloidal Stability of Silica Coated MgFe$_2$O$_4$ MNPs

For biomedical applications, MNPs should form stable dispersion in physiological saline medium like water or phosphate buffer saline (PBS). The stabilization of the MNPs is crucial to obtain magnetic colloidal ferrofluids that are stable against aggregation both in a biological medium and in a magnetic field [48]. The colloidal stabilities of the bare and silica coated sample in water and the colloidal stabilities of the coated samples in PBS (pH 5.0 and 7.4) were evaluated by the zeta potential measurements. Colloidal stability in physiological media like PBS is also useful to evaluate the strength of coating [49]. The zeta potential value in distilled water observed for the coated sample (-15.50 mV) is higher than the bare sample (-2.45 mV). The results imply that the aggregation of the coated sample in water is far less than the uncoated sample, which improves colloidal stability with increasing zeta potential values [7]. Also, enhanced zeta potential values for coated particles suggest that the silica particles have been successfully bound with surfaces of uncoated particles [50]. The negative zeta potential helps to repel each particle in the suspension, ensuring long-term stability and avoiding particle agglomeration [51]. The pH dependent zeta potentials of the coated sample is -29.15 mV at pH 7.4 (physiological pH) and -19.35 mV at pH 5.0 (cancer cell endosomal pH). The results show that the silica coated MgFe$_2$O$_4$ MNPs are colloidally stable both in physiological and inside the cancer cell environments. Colloidal stability is a very important requirement for MNPs used in biomedical applications because aggregates can cause serious harm to the patient e.g., by clogging blood vessels. These results imply that the silica coated MgFe$_2$O$_4$ MNPs could maintain their dispersion stability and heating capacity in various physiological environments and thus have great potential to be used in magnetic fluid hyperthermia as a heating mediator and as a drug delivery vehicle. However, further experiments like hemocompatibility assay, cytotoxicity tests and magnetic hyperthermia measurements have to be carried out to test their real therapeutic potentials.

4.0 Conclusion

In conclusion, the single cubic spinel phase of nanocrystalline MgFe$_2$O$_4$ MNPs was obtained by the solution combustion synthesis using a combination of urea and ammonium acetate fuels followed by annealing at 900°C for 2hrs. The surfaces of the synthesized MNPs were modified with silica for the purpose of enhanced colloidal stability for potential use in biomedical applications. FESEM, EDAX, FTIR and thermal analysis showed that the MgFe$_2$O$_4$ MNPs were successfully coated by silica. XRD revealed that the cubic spinel crystalline structure was retained in the coated samples but with slight suppression of the peaks; and there was a reduction of the crystallite sizes in the coated sample (47 nm) compared with the bare sample (53 nm). This decrease in crystallite size was generally attributed to lesser agglomeration of particles due to silica coating and to the size selection done before silica coating. The magnetic results show that MgFe$_2$O$_4$ MNPs (bare and silica coated) is ferrimagnetic at room temperature. A reduction in the magnetic properties of all the silica coated samples was observed and it was attributed to the presence of diamagnetic silica coatings and the lesser amount of magnetic substance per gram in the silica coated sample compared with the bare sample. The magnetic measurements of MgFe$_2$O$_4$ MNPs showed that the magnetic responses are frequency dependent even with silica coatings and this is an important parameter in hyperthermia and targeted drug delivery applications. Zeta potential studies revealed that there is enhanced colloidal stability of MgFe$_2$O$_4$ MNPs after silica coating in aqueous media. Also, the colloidal stability of silica coated MgFe$_2$O$_4$ MNPs in physiological media (PBS) highlights their potential applications in biomedical field.

References

[1] L. Brannon-Peppas, J.O. Blanchette, Nanoparticle and targeted systems for cancer therapy, Advanced Drug Delivery Reviews 56 (2004) 1649-1659.

[2] E.S. Kawasaki, A. Player, Nanotechnology, Nanomedicine and the Developmentof New Effective Therapies for Cancer, Nanomedicine 1 (2005) 101-109.

[3] M.M. Yallapu, F.S. Othman, E.T. Curtis, B.K. Gupta, M. Jaggi, S.C. Chauhan, Multifunctional Magnetic Nanoparticles for Magnetic Resonance Imaging and Cancer Therapy, Biomaterials 32 (2011) 1890-1905.

[4] M. Namdeo, S. Saxena, R. Tankhiwale, M. Bajpai, Y.M. Mohan, S.K. Bajpai, Magnetic Nanoparticles for Drug Delivery Applications, Journal of Nanoscience and Nanotechnology 8 (2008) 3247-3271.

[5] S.A. Shah, M.H. Asdi, M.U. Hashmi, M.F. Umar, S. Awan, Thermoresponsive Copolymer Coated $MnFe_2O_4$ Magnetic Nanoparticles for Hyperthermia Therapy and Controlled Drug Delivery, Materials Chemistry and Physics 137 (2012) 365-371.

[6] C. Wilhelm, J.P. Fortin, F. Gazeau, Tumour Cell Toxity of Intracellular Hyperthermia Mediated by Magnetic Nanoparticles, Journal of Nanoscience and Nanotechnology 7 (2007) 2933-2937.

[7] N.D. Thorat, S.V. Otari, R.A. Bohara, H.M. Yadav, V.M. Khot, A. B. Salunkhe, M.R. Phdatre, A.I. Prasad, R.S. Ningthoujam, S.H. Pawar, Structured Superparamagnetic Nanoparticles for High Performance Mediator of Magnetic FluidHyperthermia: Synthesis, Colloidal Stability and Biocompatibility Evaluation. Materials Science and Engineering C 42 (2014) 637-646.

[8] N. Kohler, C. Sun, A. Fichtenholtz, J. Gunn, C. Fang, M. Zhang, Methotrexate-Immobilised Poly (Ethylene Glycol) Magnetic Nanoparticles in MR Imaging and Drug Delivery, Small 2 (2006) 785-792.

[9] C. Sun, J.S. Lee, M. Zhang, Magnetic Nanoparticles in MR Imaging and Drug Delivery, Advanced Drug Delivery Reviews 60 (2008) 1252-1265.

[10] I.J. Bruce, T. Sen, Surface Modification of Magnetic Nanoparticles with Alkoxysilanes and Their Application in Magnetic Bio-separations, Langmuir 21 (2005) 7029-7035.

[11] C. Wilhelm, F. Gazeau, Universal Cell Labelling with Anionic Magnetic Nanoparticles, Biomaterials 29 (2008) 3161-3174.

[12] T. Osaka, T. Matsunaga, T. Nakanishi, A. Arakaki, D. Niwa, H. Iida, Synthesis of Magnetic Nanoparticles and their Application to Bioassays, Analytical and Bioanalytical Chemistry 384 (2006) 593-600.

[13] D.K. Kim, Characterization and MRI study of surfactant-coated superparamagnetic nanoparticles administrated into the rat brain, J. Magn. Magn. Mater. 225 (2001) 256–261.

[14] K. Cheng, S. Peng, C. Xu, S. Sun, Porous hollow Fe(3)O(4) nanoparticles for targeted delivery and controlled release of cisplatin, J. Am. Chem. Soc. 131 (2009) 10637– 10644.

[15] A. Makridis, K. Topouridou, M. Tziomaki, D. Sakellari, K. Simeonidis, M. Angelakeris, M.P. Yavropoulou, J. G. Yovos, O. Kalogirou, *In vitro* application of Mn-ferrite nanoparticles as novel magnetic hyperthermia agents, J. Mater. Chem. B 2 (2014) 8390-8398.

[16] R. Hiergeist, W. Andra, N. Buske, R. Hergt, I. Hilger, U. Richter, W. Kaiser, Application of magnetite ferrofluids for hyperthermia, Journal of Magnetism and Magnetic Materials 201 (1999) 420-422.

[17] P. Sivakumar, R. Ramesh, A. Ramanand, S. Ponnusamy, C. Muthamizhchelvan, Preparation of sheet like polycrystalline $NiFe_2O_4$ nanostructure with PVA matrices and their properties, Materials Letters, 65 (9) 2011 1438–1440.

[18] M. Rabanal, A. Várez, B. Levenfeld, J. Torralba, Magnetic properties of Mg-ferrite after milling process, J. Mater. Process. Technol., 143 (2003) 470-474.

[19] Q. Chen, A. J. Rondinone, B. C. Chakoumakos, Z. John Zhang, Synthesis of superparamagnetic $MgFe_2O_4$ nanoparticles by coprecipitation, Journal of Magnetism and Magnetic Materials, 194(1) (1999) 1–7.

[20] N. Kaur, M. Kaur, Comparative studies on impact of synthesis methods on structural and magnetic properties of magnesium ferrite nanoparticles, Processing and Application of Ceramics 8(3) (2014) 137–143.

[21] J. Chandradass, A. H. Jadhav, K. H. Kim, H. Kim, Influence of processing methodology on the structural and magnetic behavior of $MgFe_2O_4$ nanopowders, Journal of Alloys and Compounds, 517 (2012) 164–169.

[22] T. Sasaki, S. Ohara, T. Naka, J. Vejpravova, V. Sechovsky, M. Umetsu, S. Takami, B. Jeyadevan, T. Adschiri, Continuous synthesis of fine $MgFe_2O_4$ nanoparticles by supercritical hydrothermal reaction, J. Supercrit. Fluids, 53(3) (2010) 92-94.

[23] P. Tartaj, M. Morales, S. Veintemillas-Verdaguer, T. Gonzalez-Carreno, C.J. Serna, The Preparation of Magnetic Nanoparticles for Applications in Biomedicine, Journal of Physics D: Applied Physics 36 (2003) R182-R197.

[24] M.R. Phadatare, V.M. Khot, A.B. Salunkhe, N.D. Thorat, S.H. Pawar, Studies on Polyethylene Glycol Coating on $NiFe_2O_4$ Nanoparticles for Biomedical Applications, Journal of Magnetism and Magnetic Materials 324 (2012) 770–772.

[25] V. Uskokovic, A. Kosak, M. Drofenik, Preparation of Silica-Coated Lanthanum Strontium Manganite Particles with Designable Curie Point for Application in Hyperthermia Treatments, International Journal of Applied Ceramic Technology 3 (2): (2006) 134–143.

[26] A. Villanueva, P. de la Presa, J.M. Alonso, T. Rueda, A. Martınez, P. Crespo, M.P. Morales, M.A. Gonzalez-Fernandez, J. Valde´s, G. Rivero, Hyperthermia HeLa Cell Treatment with Silica-Coated Manganese Oxide Nanoparticles, The Journal of Physical Chemistry C 114 (2010) 1976–1981.

[27] B. Mojic, K.P. Giannakopoulos, Z. Cvejic, V.V. Srdic, Silica coated ferrite nanoparticles: Influence of citrate functionalization procedure on final particle morphology. Ceramics International 38 (2012) 6635 – 6641.

[28] S. Makhluf, R. Dror, Y. Nitzan, Y. Abramovich, R. Jelinek, A. Gedanken, Microwave-Assisted Synthesis of Nanocrystalline MgO and its use as a Bacteriocide. Advanced Functional Materials 15 (10) (2005) 1708-1715.

[29] K. Krishnamoorthy, G. Manivannan, S.J. Kim, K. Jeyasubramanian, M.J. Premanathan, Antibacterial Activity of MgO Nanoparticles Based on Lipid Peroxidation by Oxygen Vacancy, Journal of Nanoparticle Research 14 (2012) 1063-1068.

[30] S. Kanagesan, M. Hashim, S. Tamilselvan, N.B. Alitheen, I. Ismail, G. Bahmanrokh, Cytotoxic Effect of Nanocrystalline $MgFe_2O_4$ Particles for Cancer Cure, Journal of Nanomaterials (2013) 1-8.

[31] V.M. Khot, A.B. Salunkhe, N.D. Thorat, M.R. Phadatare, S.H. Pawar, Induction heating studies of combustion synthesized $MgFe_2O_4$ nanoparticles for hyperthermia applications, Journal of Magnetism and Magnetic Materials 332 (2013) 48–51.

[32] C.R. Vestal, Z.J. Zhang, Effects of surface coordination chemistry on the magnetic properties of MnFe2O4 spinel ferrite nanoparticles, J. Am. Chem. Soc., 125 (2003) 9828–9833.

[33] M. Mahdavi, F. Namvar, M.B. Ahmad, R. Mohamad, Green Biosynthesis and Characterization of Magnetic Iron Oxide (Fe_3O_4) Nanoparticles Using Seaweed (*Sargassum muticum*) Aqueous Extract, Molecules 18 (2013) 5954–596.

[34] C.O. Ehi-Eromosele, B.I. Ita, E.E.J. Iweala, Synthesis, Microstructure and Magnetic Properties of Nanocrystalline $MgFe_2O_4$ Particles: Effect of Mixture of Fuels and Sintering Temperature, Science of Sintering (Accepted for publication).

[35] W. Stober, A. Fink, E. Bohn, Controlled growth of monodisperse silica spheres in micron size range, J. Colloid Interface Sci., 26 (1968) 62–69.

[36] J. Choi, J.C. Kim, Y.B. Lee, I.S. Kim, Y.K. Park, N.H. Hur, Fabrication of Silica-Coated Magnetic Nanoparticles with Highly Photoluminescent Lanthanide Probes. Chemical Communications 16 (2007) 1644-1646.

[37] A.B. Salunkhe, V.M. Khot, N.D. Thorat, M.R. Phadatare, C.I. Sathish, D.S. Dhawale, S.H. Pawar, Polyvinyl Alcohol Functionalized Cobalt Ferrite Nanoparticles for Biomedical Applications, Applied Surface Science 264 (2013) 598-604.

[38] B. Zhou, Y.W. Zhang, C.S. Liao, C.H. Yan, L.Y. Chen, S.Y. Wang, Rare Earth Mediated Magnetism and Magneto-Optical Kerr Effects in Nanocrystalline $CoFeMn_{0.9}RE_{0.1}O_4$ Thin Films, Journal of Magnetism and Magnetic Materials 280 (2004) 327–333.

[39] H.M. Zaki, H.A. Dawoud, Far-infrared Spectra for Copper–Zinc Mixed Ferrites, Physica B 405 (2010) 4476–4479.

[40] A. Venkateswara Rao, P.B. Wagh, D. Haranath, P.P. Risbud, S.D. Kumbhare, Influence of Temperature on the Physical Properties of TEOS Silica Xerogels, Ceramic International 25 (6): (1999) 505–509.

[41] K.H. Wu, W.C. Huang, Effect of Varying the Acid to Metal Ion Ratio R on the Structural and Magnetic Properties of SiO_2-Doped Ni–Zn Ferrite, Journal of Solid State Chemistry 177 (2004) 3052–3057.

[42] B. Topuz, D. Şimşek, M. Çiftçioğlu, Preparation of monodisperse silica spheres and determination of their densification behaviour. Ceramics International 41(1) (2015) 43-52.

[43] S. Zellmer, M. Lindenau, S. Michel, G. Garnweitner, C. Schilde, Influence of surface modification on structure formation and micromechanical properties of spray-dried silica aggregates. J Colloid Interface Sci. 464 (2016) 183-190.

[44] C.P. Liu, M.W. Li, Z. Cui, J.R. Huang, Y.L. Tian, T. Lin, W.B. Mi, Comparative study of magnesium ferrite nanocrystallites prepared by sol–gel and coprecipitation methods, J. Mater. Sci. 42 (2007) 6133-6138.

[45] V.M. Khot, A.B. Salunkhe, M.R. Phadatare, S.H. Pawar, Formation, Microstructure and Magnetic Properties of Nanocrystalline $MgFe_2O_4$, Materials Chemistry and Physics 132 (2012) 782–787.

[46] A.B. Salunkhe, V.M. Khot, M.R. Phadatare, N.D. Thorat, R.S. Joshi, H.M. Yadav, S.H. Pawar, Low Temperature Combustion Synthesis and Magnetostructural Properties of Co-Mn Nanoferrites, Journal of Magnetism and Magnetic Materials 352 (2014) 91-98.

[47] M. Rahimi, P. Kameli, M. Ranjbar, H. Salamati, The Effect of Polyvinyl Alcohol (PVA) Coating on Structural, Magnetic Properties and Spin Dynamics of $Ni_{0.3}Zn_{0.7}Fe_2O_4$ Ferrite Nanoparticles, Journal of Magnetism and Magnetic Materials 347 (2013) 139–145.

[48] E. Umut, Surface Modification of Nanoparticles used in Biomedical Applications In: Modern Surface Engineering Treatments, Ed. by Mahmood Aliofkhazraei, InTech (2013) 185-208.

[49] N.D. Thorat, V.M. Khot, A.B. Salunkhe, A. Prasad, R.S. Ningthoujam, S.H. Pawar, Surface Functionalized LSMO Nanoparticles with Improved ColloidalStability for Hyperthermia Applications, Journal of Physics D: Applied Physics 46 105003 (2013) 1-11.

[50] S.V. Jadhav, D.S. Nikam, V.M. Khot, S.S. Mali, C.K. Hong, S.H. Pawar, PVA and PEG Functionalised LSMO Nanoparticles for Magnetic Fluid Hyperthermia Application, Materials Characterization 102 (2015) 209–220.

[51] P. Smirnov, Cellular Magnetic Resonance Imaging using Superparamagnetic Anionic Iron Oxide Nanoparticles: Applications to *In Vivo* Trafficking of Lymphocytes and Cell-Based Anticancer Therapy, Methods in Molecular Biology 512 (2009) 333-353.